HHS Public Access

Author manuscript

Am J Surg Pathol. Author manuscript; available in PMC 2019 May 01.

Published in final edited form as:

Am J Surg Pathol. 2018 May ; 42(5): 604–615. doi:10.1097/PAS.0000000000000965.

BCOR-CCNB3-Fusion Positive Sarcomas: A Clinicopathologic and Molecular Analysis of 36 cases with Comparison to Morphologic Spectrum and Clinical Behavior of other Round Cell Sarcomas

Yu-Chien Kao, MD[1,2], **Adepitan A. Owosho, DDS**[3,4], **Yun-Shao Sung, MSc**[1], **Lei Zhang, MD**[1], **Yumi Fujisawa, MS**[1], **Jen-Chieh Lee, MD, PhD**[5], **Leonard Wexler, MD**[6], **Pedram Argani, MD**[7], **David Swanson, BSc**[8], **Brendan C Dickson, MD**[8], **Christopher D.M. Fletcher, MD, FRCPath**[9], and **Cristina R Antonescu, MD**[1,*]

[1]Department of Pathology, Memorial Sloan Kettering Cancer Center, New York, NY, USA

[2]Department of Pathology, Shuang Ho Hospital, Taipei Medical University, Taipei, Taiwan

[3]Department of Surgery, Memorial Sloan Kettering Cancer Center, New York, NY, USA

[4]College of Dental Medicine, University of New England, Portland Maine, USA

[5]Department and Graduate Institute of Pathology, National Taiwan University Hospital, National Taiwan University College of Medicine, Taiwan

[6]Department of Pediatrics, Memorial Sloan Kettering Cancer Center, New York, NY, USA

[7]Departments of Pathology, The Johns Hopkins Medical Institutions, Baltimore, MD, USA

[8]Department of Pathology & Laboratory Medicine, Mount Sinai Hospital, Toronto, Canada

[9]Department of Pathology, Brigham and Women's Hospital, Harvard Medical School, Boston, MA, USA

Abstract

BCOR-CCNB3 sarcoma (BCS) is a recently defined genetic entity among undifferentiated round cell sarcomas, which was initially classified as and treated similarly to the Ewing sarcoma (ES) family of tumors. In contrast to ES, BCS shows consistent BCOR overexpression, and preliminary evidence suggests that these tumors share morphologic features with other tumors harboring *BCOR* genetic alterations, including *BCOR* internal tandem duplication (ITD) and *BCOR-MAML3*. To further investigate the pathologic features, clinical behavior, and their relationship to other round cell sarcomas, we collected 36 molecularly confirmed *BCOR-CCNB3* sarcomas for a detailed histologic and immunohistochemical analysis. Four of the cases were also analyzed by RNA sequencing. An additional case with BCOR overexpression but negative *CCNB3* abnormality showed a novel *KMT2D-BCOR* fusion by targeted RNA sequencing. The patients ranged in age from 2 to 44 years old (mean: 14.8; median: 15), with striking male predominance

[*]**Corresponding Author:** Cristina R Antonescu, MD, Memorial Sloan-Kettering Cancer Center, Department of Pathology, 1275 York Ave, New York, NY, 10065; Phone: (212) 639-5905; antonesc@mskcc.org.

Conflicts of interest: none

(M:F=31:5). The tumor locations were slightly more common in bone (n=20) than soft tissue (n=14), with rare visceral (kidney, n=2) involvement. Histologically, BCS showed a spectrum of round to spindle cells with variable cellularity, monomorphic nuclei and fine chromatin pattern, delicate capillary network, and varying amounts of myxoid or collagenous stroma. The morphologic features and immunoprofile showed considerable overlap with other round cell sarcomas with *BCOR* oncogenic up-regulation, i.e. *BCOR-MAML3* and *BCOR* ITD. Follow-up available in 22 patients showed a 5-year overall survival of 72%, which was relatively similar to ES (79%, p-value=0.738) and significantly better than *CIC-DUX4* sarcomas (43%, p-value=0.005) control groups. Local recurrences occurred in 6 patients and distant metastases (lung, soft tissue/bone, pancreas) in 4. Seven of 9 cases treated with an ES chemotherapy regimen with evaluable histologic response showed >60% necrosis in post-therapy resections. Unsupervised clustering by RNA sequencing data revealed that tumors with *BCOR* genetic alterations, including *BCOR-CCNB3, BCOR-MAML3* and *BCOR* ITD, formed a tight genomic group distinct from ES and *CIC*-rearranged sarcomas.

Keywords

round cell sarcoma; Ewing sarcoma; *BCOR*; *CCNB3*; fusions

INTRODUCTION

BCOR-CCNB3 sarcomas (BCS) were first identified by Pierron et al in 2012 among a large group of undifferentiated round cell sarcomas lacking known genetic alterations through a whole transcriptome sequencing and subsequent RT-PCR screen.[1] The genetic abnormality involves a paracentric inversion on the short arm of chromosome X, resulting in the fusion of 2 nearby genes *BCOR* and *CCNB3* (10 Mb apart) and leading to the overexpression of CCNB3. This initial study showed that BCS occurs with predilection in male adolescents and skeletal locations and has a primitive round cell morphology reminiscent of Ewing sarcomas (ES).[1] Two subsequent smaller series of 10 and 6 cases, respectively, pointed out these tumors harbor a mixed round to spindle cell morphology and are evenly distributed between bone and soft tissue sites.[2,3] Based on these findings, the differential diagnosis of BCS is quite challenging, including not only tumors in the ES family but also undifferentiated spindle cell sarcomas, such as synovial sarcomas (SS) and malignant peripheral nerve sheath tumors (MPNST). Because of the common presentation within bone, BCS can be further confused with small cell osteosarcoma. Thus in most cases a molecular diagnosis demonstrating the presence of *BCOR-CCNB3* fusion is required for a more definitive diagnosis. More recently, emerging evidence suggested that tumors with *BCOR* genetic abnormalities, including *BCOR-CCNB3, BCOR-MAML3* and *BCOR* ITD (internal tandem duplications) share significant overlap not only at the gene expression level, due to BCOR up-regulation, but also morphologically.[4] This study sets out to define the morphologic and immunohistochemical spectrum of a large cohort of molecularly confirmed BCS and evaluate features that overlap with other members of the so-called ‘BCOR family of tumors’. Furthermore, as these tumors have been managed with similar chemotherapy regimens to those used in ES, we also examined the therapy-related pathologic response in

our cohort and compared the survival of the BCS study group to individual cohorts of molecularly defined ES, *CIC-DUX4* sarcoma and SS.

MATERIALS AND METHODS

Study cohort

The Surgical Pathology files of MSKCC as well as the consultation files of the senior authors (C.R.A., C.D.M.F., B.C.D.) were searched for primitive round and spindle cell sarcomas that had molecular confirmation of *BCOR-CCNB3* fusion by fluorescence in situ hybridization (FISH) or RNA sequencing (RNAseq). Hematoxylin and eosin stained slides were reviewed. Cases without available material for review were excluded. Three cases were reported previously (cases 18, 21, 27).[5,6] The study group was analyzed for demographic information, anatomic site, tumor size, and morphologic features, including cell type (round, spindle, mixed), degree of cellularity, type and amount of stromal component, nuclear features, mitotic activity and presence of necrosis. Available immuno-histochemical stains were reviewed, including BCOR, SATB2, cyclin D1, TLE1, Bcl-2, and CD99. The clinical follow-up information was obtained from review of the electronic medical records and from contacting referring pathologists and clinicians. The study was approved by the Institutional IRB.

Fluorescence in situ hybridization (FISH)

FISH for *BCOR-CCNB3* fusions was performed on 4-μm formalin-fixed paraffin-embedded tissue sections in 34 cases. Custom FISH probes were prepared using bacterial artificial chromosomes (BAC) flanking *BCOR* (telomeric: RP11-21D3, RP11-1105N2; centromeric: RP11-37K20, RP11-973F20) and *CCNB3* (telomeric: RP11-58H17; centromeric: RP11-168F22, RP11-96H3). The FISH procedure was performed as previously described.[7]

RNA sequencing (RNAseq)

One and three cases were submitted to whole transcriptome sequencing (case 19) and targeted RNAseq (case 8, 21, 35), respectively. For whole transcriptome sequencing, total RNA was extracted from frozen tissues using RNeasy Plus Mini (Qiagen), followed by mRNA isolation with oligo(dT) magnetic beads and fragmentation by incubation at 94°C in fragmentation buffer (Illumina) for 2.5 minutes. After gel size-selection (350–400bp) and adapter ligation, the library was enriched by PCR for 15 cycles and purified. Paired-end RNAseq at read lengths of 50 or 51 bp was performed with the HiSeq 2000 (Illumina). For targeted RNAseq, RNA was extracted from FFPE tissue using Amsbio's ExpressArt FFPE Clear RNA Ready kit (Amsbio LLC, Cambridge, MA). Fragment length was assessed with an RNA 6000 chip on an Agilent Bioanalyzer (Agilent Technologies, Santa Clara, CA). RNAseq libraries were prepared using 20–100 ng total RNA with the Trusight RNA Fusion Panel (Illumina, San Diego, CA), which targets a list of 507 genes of interest. Targeted RNAseq was performed on an Illumina MiSeq platform. Reads were independently aligned with STAR(ver 2.3) against the human reference genome (hg19) and analyzed by STAR-Fusion.

Reverse transcription-polymerase chain reaction (RT-PCR)

RT-PCR was performed in case 19 to validate the fusion transcript identified by RNAseq. RNA was extracted from frozen tissues by RNeasy Plus Mini (Qiagen) and reverse transcribed by SuperScript IV First-Strand Synthesis System (Invitrogen). PCR was performed by Advantage 2 PCR kit (Clontech, Mountain View, CA). Forward BCOR primer (5'-GACCTGGAAGCCTTCAACCC) and reverse CCNB3 primer (5'-GAAGAGAGATGCCTCCTCAGTG) were used. The reaction was run at an annealing temperature of 66°C for 35 cycles.

Expression profile analysis by Affymetrix U133A Plus 2 array

To compare the expression profile of *BCOR-CCNB3* sarcomas (BCS) with morphologically similar tumors, including ES and SS, we have downloaded publicly available expression array data from GEO, including: 10 BCS (GSE34800) and 4 ES (GSE34800) from the study by Pierron et al,[1] 34 SS (GSE20196),[8] and a control group of normal tissues (GSE7307) on Affymetrix Human Genome U133A Plus 2 platform. Gene signatures of each tumor entity were obtained by comparing to a control group of normal tissues, using log2-fold change threshold of positive 3 and negative 5, FDR 0.01. A Venn diagram was used to assess the relationship among these gene signatures. Supervised clustering was performed using the gene signature specific for each group.

Due to the overrepresentation of multiple *HOX* family genes in the signature of BCS, we further examined the expression of *HOX* genes in BCS, ES, SS (Affymetrix U133A Plus 2 array), *BCOR* ITD round cell sarcoma, and *CIC*-rearranged sarcoma (RNAseq data). The expression fold changes between each tumor type compared to the appropriate control groups (normal tissues for the Affymetrix array; various soft tissue tumors for the RNAseq dataset) were evaluated in each dataset.

Survival analysis

Follow-up data were available in 22 BCS patients. Statistical analysis was performed on an SPSS platform (version 24.0; IBM Corp., Armonk, NY). The overall survival (OS) time was measured in months from the date of diagnosis to the date of death. Kaplan-Meier estimate was used to calculate the OS. Survival data of 57 *CIC*-rearranged round cell sarcomas, 121 ES, and 34 head and neck SS from our previous studies were used for comparison.[9,10] The OS among different tumors were compared by log-rank analysis. A $P<0.05$ was considered as significant for all statistical analyses.

RESULTS

BCOR-CCNB3 sarcomas affect mainly male adolescents with slight preference for bone location

The study cohort of 36 patients showed a striking male predominance (31/36, 86%). The age at presentation ranged from 2 to 44 years old (mean & median: 15)(Table 1), with 81% of cases occurring between 10–20 years of age. The tumor locations were distributed between bone (n=20) and soft tissue (n=14), with rare visceral involvement (n=2). Axial locations and extremities were equally involved. Among skeletal lesions, femur was the most common

single site (n=5), followed by tibia (n=4), while all the axial skeletal tumors involved pelvic bones (3 in sacrum, 2 in ilium, 2 in pubic ramus). Soft tissue lesions occurred within trunk (n=7), extremities (n=4), and head and neck (n=3). Kidney was the only visceral location identified in this cohort. The tumor sizes ranged from 3–27 cm (mean: 11.7; median: 11).

BCOR-CCNB3 sarcomas showed a wide morphologic spectrum ranging from round to spindle cell phenotype

The majority of cases (28, 78%) were composed predominantly of primitive round cells, while 8 (22%) cases showed mainly spindle cell morphology. Two-thirds of BCS with predominant round cell phenotype (19 cases) also had a minor ovoid to spindle cell component, while 3 of the 8 predominantly spindle cell BCS showed a minor round cell component. The round cell component had scant cytoplasm and monomorphic nuclei with fine chromatin, indistinct nucleoli, and smooth nuclear contours (Fig. 1A). The tumor cells were usually arranged in solid hypercellular sheets without a distinct architectural pattern. At the other end of the spectrum were tumors composed predominantly or exclusively of monomorphic spindle cells, commonly arranged in intersecting fascicles (Fig. 1B) and less often in a vague whorling pattern (Fig. 1C). Most of these spindle cell lesions showed medium to high cellularity, monomorphic, ovoid nuclei with similar fine chromatin pattern. Regardless of the round or spindle cell morphology, most of the tumors showed a rich capillary network (81%). One case revealed alternating low and high cellularity with perivascular condensation, reminiscent of the so-called ‘marbled pattern’ commonly seen in malignant peripheral nerve sheath tumor (MPNST)(Fig. 1D). Half of the cases showed some degree of myxoid stroma (n=19, 53%), either loosely separating small nests, cords or individual tumor cells, or forming a microcystic pattern (Fig. 1E–H). In some cases, an abrupt transition between hypercellular and hypocellular myxoid areas were noted (Fig. 1I). A third of cases (n=13, 36%) showed a more collagenous stroma, either as ropey collagen bundles separating individual tumor cells or as a more confluent collagenous stroma in areas of lower cellularity (Fig. 2A,B, D–F). Metaplastic ossification was noted in a metastatic lung lesion in one case (Fig. 2C). Necrosis, either focal or geographic, was present in 16 (44%) cases. Mitotic activity varied significantly, ranging from 1–25/10 high power fields (HPFs) (mean: 8; median: 6).

Two cases showed a deceptively bland and hypocellular spindle cell morphology in the primary lesion, but recurred as a highly cellular round cell sarcomas. One of them, a markedly cystic kidney tumor in a 12 year-old male patient, has been reported previously.[6] The other case (case # 20) was a 14 year-old male who presented with a progressively enlarging and tender right 5th toe mass, centered in the soft tissue and showing phalangeal bone destruction. The excised primary lesion was composed of relatively bland-spindle cells with low to medium cellularity, and associated with a collagenous to hyalinized stroma (Fig. 2G–H). Mitotic activity was low (1/10HPFs). BCOR immunostaining showed patchy moderate to strong staining (Fig. 2H, inset). The surgical margin was involved by the tumor and the patient underwent post-operative radiation therapy. One year later, the patient developed a local recurrence involving mainly the phalangeal bone. A wide excision was performed and showed a predominantly round cell sarcoma (Fig. 2I) with only focal spindle

cell morphology, similar to the primary lesion. Both the primary and recurrent specimens were positive for *BCOR-CCNB3* fusion by FISH.

BCOR-CCNB3 fusions identified by FISH and RNA sequencing

All except 2 cases were tested by FISH using the 3-color *BCOR-CCNB3* fusion assay. FISH results typically showed inversions of both *BCOR* and *CCNB3* and fusion of centromeric *BCOR* (5') to centromeric *CCNB3* (3') (Fig. 3A,B). In some cases, additional unbalanced alterations were observed, such as deletion of telomeric *BCOR* (3') signals, additional regional breaks, or deletion of the other allele.

Four cases evaluated by RNAseq confirmed the *BCOR-CCNB3* fusion, with a similar *BCOR* exon 15 to *CCNB3* exon 5 transcript as previously reported (Fig. 4A).[1] The fusions were further confirmed by RT-PCR in 1 case (Fig. 3C). Akin to sarcomas with *BCOR-MAML3* and *BCOR* ITD, the *BCOR* genetic abnormality consistently involves the end of the last exon of *BCOR* (exon 15)(Fig. 4A).[4,11] Marked mRNA up-regulation of the entire *BCOR* coding sequence was noted in both *BCOR-CCNB3* and *BCOR* ITD tumors (Fig. 4B). In contrast, *CCNB3* mRNA up-regulation was noted only in BCS, involving the distal part of the gene, after the exon 5 breakpoint (data not shown). By unsupervised clustering, BCS grouped together with *BCOR* ITD and *BCOR-MAML3* tumors and was separated from ES and *CIC*-rearranged sarcomas (Fig. 4C).

A novel *KMT2D-BCOR* identified by targeted RNA sequencing in a recurrent pelvic soft tissue mass

An additional round cell sarcoma, showing diffuse and strong positivity for BCOR and moderate staining for SATB2, while being negative for *BCOR-CCNB3* fusion by FISH, was investigated by targeted RNA sequencing. The lesion presented as a large pelvic soft tissue mass (size: 11 cm) in a 10 year-old female. Microscopically, the tumor showed a round to short spindle cell phenotype, arranged in short fascicles and whorling pattern. RNAseq identified *KMT2D-BCOR* gene fusion with multiple breakpoints, including the reciprocal transcript (*BCOR-KMT2D*). The most abundant fusion junction read was *KMT2D* exon 42 to the last 173 bp of *BCOR* exon 4. *BCOR* mRNA expression was up-regulated, especially involving the 3' exons of *BCOR* gene, distal to the breakpoint, supporting *BCOR* as the 3' partner. The patient was treated with initial debulking surgery followed by chemotherapy, and subsequent re-excision showed rare microscopic residual foci of viable tumor (>90% chemotherapy response). The tumor recurred locally two years later.

BCS shares a similar immunoprofile with other tumors harboring *BCOR* genetic alterations

All BCS tested showed nuclear positivity for BCOR (18/18), typically with a strong and diffuse nuclear pattern (Fig 5A). BCOR expression was retained in the residual viable tumor in a post-chemotherapy resection, showing >90% tumor necrosis/fibrosis (Fig. 5B). In addition, most tumors were positive for SATB2 (10/12, 83%), cyclin D1 (9/10, 90%), TLE1 (8/10, 80%) and Bcl-2 (7/7, 100%)(Fig. 5C–E). The consistent immunoreactivity for these markers matched the mRNA up-regulation at gene expression level (data not shown). CD99 was only positive in about half of the cases (11/26, 42%) with variable intensity and extent.

In addition, *NTRK3* was identified as one of the differentially expressed genes in *BCOR-CCNB3* tumors.

Distinctive *HOX* gene family up-regulation in sarcomas with *BCOR* genetic alterations

By Affymetrix U133A array data analysis, BCS showed up-regulation of multiple members of the *HOX* gene family, including *HOXA, HOXB, HOXC*, and to a lesser extent *HOXD* (Supplementary Fig. 1). Some SS also showed HOX gene expression, especially for *HOXD* genes; while only occasional, non-recurrent *HOX* gene expression was noted in the 4 ES samples. Using RNAseq data, we found that *HOX* genes were also up-regulated in *BCOR* ITD tumors, especially for *HOXA* and *HOXB*, but not in *CIC*-rearranged sarcomas (Supplementary Fig. 1). Overall, both BCS and *BCOR* ITD tumors showed distinctive overexpression of multiple *HOX* genes. Similar results were previously shown by our group in round cell sarcomas with *BCOR-MAML3* fusion.[11]

Furthermore, we obtained the individual gene expression signatures of BCS (249 genes), ES (93 genes), and SS (150 genes) from Affymetrix U133A array data, as described above. A Venn diagram showed an overlap of 11 genes between the 3 sarcoma types, including *EZH2, WNT5A*, and *PMP2 (peripheral myelin protein 2)*, with most of the remaining genes representing distinctive signatures for each subtype (Fig. 6A). Supervised clustering was performed using the BCS gene signature, showing distinctly separate groups of BCS, ES and SS samples (Fig. 6B).

BCOR-CCNB3 sarcomas have a significantly better outcome than *CIC*-rearranged sarcomas

Twenty-two BCS patients with available follow-up were analyzed and compared to previously published data sets of localized ES, *CIC*-rearranged sarcomas, and head and neck SS.[9,10] The average follow-up duration of the study group was 38 months (range: 7–113 months). All except one patient with available follow-up presented with localized disease at diagnosis, while the remaining patient (17/M) with a pubic ramus tumor and soft tissue extension was found to have a pancreatic metastasis at diagnosis. During the follow-up period, 6 patients developed local recurrence and 3 distant metastases (Table 1). Metastatic sites included lung (n=3), skull base, pelvis, scapula, and thigh (n=1 each).

Of the 22 patients, 11 received neoadjuvant chemotherapy/chemoradiation followed by surgery, 7 had surgery followed by adjuvant chemotherapy, 1 chemotherapy, and 4 surgery alone. Most of the patients treated with chemotherapy were based on protocols for ES (Table 1). Seven of 9 patients treated with an ES chemotherapy regimen and evaluable histologic response showed significant treatment-related pathologic response (60–100% necrosis/fibrosis) in the post-therapy resection specimens. However, a recent case, not included in the survival analysis (case # 9), also treated with ES based neoadjuvant chemotherapy, showed no response. The patient underwent partial foot resection/ray amputation and post-operative radiation therapy. Lung nodules were identified radiographically.

At last follow-up, 13 patients had no evidence of disease, 6 were alive with disease, two died of disease, and one died of an unknown cause. The 3-year and 5-year survival rates were 93% and 72%, respectively. No significant prognostic difference was found in patients with

mitotic rates ≥10/10 high power fields versus those with < 10/10 high power fields (p-value=1.000). Comparing these rates to the survival of ES, *CIC*-rearranged sarcomas, and SS (a head and neck cohort), a significant survival difference was noted (Log-rank p-value <0.0001), with *CIC*-rearranged sarcomas having the worst prognosis (Fig. 7). BCS showed a significantly better prognosis than *CIC*-rearranged sarcomas (p=0.005), while no statistical difference was noted between BCS and ES (p=0.738) or between BCS and head and neck SS (p=0.802).

DISCUSSION

In this study, we investigate a series of 36 BCS for their clinicopathologic features, including the morphologic spectrum and clinical outcome. Our results confirm the male predominance and predilection for older children and adolescents as the most commonly affected population.[1] In contrast to the initial report, our series reveals only a slight preference for skeletal (56%) over soft tissue (39%) locations, with equal distribution between axial sites and extremities.[1,2] Furthermore, although initially described as a prototypical round cell sarcoma, further evidence showed that common histologic features of BCS include a mixed round, ovoid to short spindle cell phenotype, arranged in fascicles or a whorling pattern, with often myxoid stroma, and arborizing capillary network.[2,3,5,12,13] In this series, 78% of cases showed a predominant round cell component, with most displaying, in addition, variable areas of ovoid to spindle tumor cells. The remaining 22% of cases showed predominantly monomorphic spindle cell features arranged in intersecting fascicles, reminiscent of MPNST or synovial sarcoma. Immuno-histochemically, all tumors tested were positive for BCOR, while cyclin D1, SATB2 and TLE1 were also positive in the majority of cases. The morphologic spectrum and immunostaining profile highlight the significant overlap with other tumor entities sharing *BCOR* genetic alterations.

BCOR was first identified as a co-repressor of BCL6, interacting with BCL6 through its N-terminal BCL6 binding domain.[14] Subsequently, BCOR was found to be a core component of a variant PRC1.1 complex associated with chromatin remodeling and histone modification.[15] As part of the PRC1.1 complex, the C-terminal BCOR PUFD domain binds to the RAWUL domain of PCGF1.[16] Of interest, all *BCOR* genetic abnormalities implicated in sarcomagenesis, including *BCOR-CCNB3, BCOR-MAML3* and *BCOR* ITD, involve the last exon of *BCOR*, which encodes the PUFD domain.[16] Thus the formation of gene fusions and ITD may alter the binding affinity between BCOR and PCGF1, affecting the subsequent recruitment by KDM2B, ubiquitinylation of H2AK119, and downstream gene regulation.[17] Additional fusions involving *BCOR* (i.e. *ZC3H7B-BCOR*) have also been reported in endometrial stromal sarcomas and ossifying fibromyxoid tumors, where *BCOR* is often the 3' partner, contributing its exons 7–15.[18,19] *BCOR*-related translocations have also been described in hematoproliferative disorders involving different mechanisms, such as recurrent *BCOR-RARA* fusions (exon 12 of *BCOR* to exon 3 of *RARA*) in a small subset of acute promyelocytic leukemia; resulting in chimeric transcripts lack the PUFD domain at the C-terminus.[20] *BCOR* inactivating mutations have also been identified in rhabdomyosarcomas and several hematologic malignancies,[21,22] while germline *BCOR* mutation results in the oculofaciocardiodental syndrome.[23]

CCNB3 is a relatively new member of the cyclin B family involved in cell cycle control,[24] being mainly expressed in the developing germ cells in the testis. The predicted *BCOR-CCNB3* fusion oncoprotein retains the CCNB3 cyclin box, while lacking the N-terminal destruction box motif associated with CCNB3 degradation.[24] In adult human tissues, both BCOR and CCNB3 are expressed in the testis,[2,25] indicating that they may have important function in germ cell survival or development. In BCS, *CCNB3* expression is consistently up-regulated.[1]

Recent data from our group have suggested that undifferentiated sarcomas characterized by *BCOR* genetic alterations, spanning both gene fusions and ITD, share similarities at the morphologic and immunohistochemical level, despite the wide spectrum of clinical presentations and pathologic entities involved.[4,25] Although our preliminary results suggest that infantile soft tissue undifferentiated round cell tumors (URCS) with *BCOR* ITD, primitive myxoid mesenchymal tumor of infancy (PMMTI) and clear cell sarcoma of the kidney (CCSK) represent a morphologic continuum of a single pathologic entity based on the shared genetic alterations, it is less certain if sarcomas with *BCOR*-related fusions, such as *BCOR-CCNB3*, also fit within this spectrum. The present study investigating the morphologic and immunohistochemical profile of a large group of BCS further emphasizes the similarities to the *BCOR* ITD genetic group, such as URCS, PMMTI and CCSK. Despite their predilection for infants and soft tissue, infantile URCS with *BCOR* ITD or *YWHAE* fusions show striking morphologic overlap with BCS, including round to spindle cell morphology, fine chromatin pattern, rich capillary background, and myxoid stroma.[4] Additionally, BCS and *BCOR* ITD tumors show an identical immunoprofile, with strong/diffuse reactivity for BCOR, SATB2, and cyclin D1 in the majority of cases.[6,25] However, despite the close genomic grouping by RNAseq unsupervised clustering, *BCOR* ITD spectrum of tumors do not show *CCNB3* mRNA expression, a common finding in BCS. Likewise, the 2 renal BCS reported by our group recently resemble CCSK, both morphologically and immunohistochemically.[6] Being the second most common pediatric renal tumor following Wilms' tumor, CCSK typically shows uniform round to ovoid cells with fine chromatin separated by a rich vascular network and is characterized by *BCOR* ITD and *BCOR* up-regulation in the majority of cases.[26] Nevertheless, CCSK mainly affects children between 2 to 4 years old, in contrast to the teenage group of BCS.

As the majority of BCS show some evidence of spindling, with 12% of BCS harboring a predominantly spindle cell fascicular growth, the differential diagnosis of BCS also includes spindle cell sarcomas, specifically monophasic SS, fibrosarcoma and MPNST. In addition, half of SS are positive for BCOR, and both SS and BCS are immunopositive for TLE1.[25,27] SATB2 reactivity, often expressed in BCS (80%), can also be detected in a small subset of SS (12%).[25] CCNB3 staining has been reported to be negative in SS, except nonspecific cytoplasmic staining in some cases.[5] A further pitfall was recently revealed in a SS18-negative spindle cell sarcoma showing diffuse BCOR expression and morphologically suspected to represent a *BCOR*-alteration sarcoma, however, RNA sequencing found a rare *SS18L1-SSX* variant fusion, diagnostic of SS.[7]

Despite their similar clinical and demographic presentation, BCS shows histologic features distinctive from ES, including the more variable cytomorphology, from round, ovoid to

spindle, common myxoid background and a rich capillary network. In contrast, ES is usually characterized by solid sheets of perfectly monomorphic round cells, ill-defined cell borders and fine chromatin, and the lack of significant stromal component. Immunohistochemically, ES shows consistent strong and diffuse CD99 membranous staining, which is much more variable in BCS. Cyclin D1 is expressed in both ES and BCS.[28] In contrast, strong and diffuse BCOR expression is the defining feature for BCS, while being only infrequently expressed in ES (1/9, 11%).[25]

Another important differential diagnosis is with *CIC-DUX4* fusion positive undifferentiated round cell sarcoma. In contrast to BCS, *CIC*-rearranged sarcomas typically affect young adults rather than children (mean age of 32) with no gender predilection. The overwhelming majority occur in soft tissue locations with infrequent intra-osseous presentation.[9] Morphologically, *CIC*-rearranged sarcomas show a higher degree of nuclear variability, with prominent nucleoli and consistent immunoreactivity for ETV4 and WT1.[9,29]

As BCS often presents as an intra-osseous lesion with a round cell/undifferentiated phenotype, expression of SATB2 might suggest an osteoblastic line of differentiation and be misinterpreted as a small cell osteosarcoma. Indeed 2 cases in this series were initially misdiagnosed as small cell OS involving femur and tibia, respectively, both locations being common for both diagnoses.[30] Osteoid or metaplastic bone formation in BCS is rare and so far only observed in metastatic lung lesions, including the case reported in our series.[2] Thus, our results point out that SATB2 expression is not specific for bone-forming tumors, and the immunowork-up of a skeletal round cell malignancy should include, in addition to SATB2, other markers such as BCOR and cyclin D1 to exclude a BCS diagnosis.

The RNA sequencing data from the 4 BCS cases and the publicly available expression array data from the Pierron study[1] revealed significant mRNA up-regulation of *NTRK3* in BCS, which was also confirmed in a subset of our cases at the protein level (data not shown). The mechanism of *NTRK3* mRNA up-regulation remains unclear. Similar *NTRK3* overexpression is also observed in the infantile URCS with *BCOR* ITD (data not shown).

Besides the morphologic differences between BCS and other undifferentiated round to spindle cell sarcomas, such as ES, *CIC*-rearranged sarcomas, and SS, our study also addressed their clinical behavior. Previous studies suggested a 5-year overall survival rate of 75% for BCS, with axial location, local recurrence, and metastasis being poor prognostic factors.[2,12] In patients with localized disease, induction therapy with ES-based protocols was associated with a better outcome.[12] The overall survival of BCS reported in a small series of 10 patients (6 with localized stage at presentation) was not statistically different from an ES cohort.[2] However, no prior studies have compared the outcome of BCS with *CIC*-rearranged sarcomas or SS, two pathologic entities commonly included in the differential diagnoses. Our study analyzed the clinical outcome of 22 BCS patients (mean follow-up: 38 months) showing that the overall survival of BCS (3-year: 93%, 5-year: 72%), is superior to *CIC*-rearranged sarcomas, while not statistically different from ES and SS. Given that these retrospective cohorts were composed of patients treated non-uniformly in different institutions, further investigation of patients with matched risk factors, disease stages, and uniform treatment protocols would be needed to confirm this finding. An additional point of

investigation was assessing the pathologic response of BCS tumors to the applied neoadjuvant chemotherapy regimens. As BCS was originally classified among ES family of tumors, most patients have been managed so far with ES-related chemotherapy protocols. Two previous studies have suggested that BCS are chemo-responsive;[2,12] one study showing a good histologic response (>90% necrosis) in 77% (10 of 13) of the evaluable patients treated mainly with ES chemotherapy but also other regimens.[12] In another study, 4 of 6 post-chemotherapy resections showed complete response, while the remaining 2 had scattered residual tumor cells.[2] Our study has further investigated the extent of tumor response in 9 resection specimens treated with ES regimens, showing 5/9 patients with >90% necrosis and 2/9 patients with >60% necrosis. Of note, other tumors with oncogenic BCOR up-regulation, e.g. CCSK, have been treated with somewhat different chemotherapy regimens, which usually do not include ifosfamide as in most ES regimens.[31,32] Given the overlapping morphology and transcriptional profile of BCS and CCSK and given that CCSK has shown sensitivity to doxorubicin-based chemotherapy,[32,33] it remains to be determined if BCS patients might also benefit from an overall less toxic protocol compared to the presently applied ES-based regimens (doxorubicin and ifosfamide combination). Another consideration is that CCSK are well-known to relapse many (over ten) years after diagnosis, mandating long term follow-up for these children. Given the genetic relatedness of BCS and CCSK, it is possible that BCS patients may relapse late too, though there is little data to address this concern at this time.

As indicated by previous microarray data analysis[1] and our RNAseq hierarchical clustering, BCS showed a distinct transcriptional profile compared to ES. This study further demonstrated the BCS expression signature is similar to tumors harboring *BCOR* ITD and *BCOR-MAML3*, with a significant up-regulation of *HOX* (homeobox) family genes.[1,11] *HOX* genes encode a group of transcription factors responsible for embryo development, including anterior-posterior body axis, and adult fracture healing process.[34,35] HOX abnormalities have also been reported in various cancer types, including carcinomas of breast, colon, prostate, and lung.[36] In sarcomas, overexpression of *HOX* genes has been reported in ES,[34] but restricted to *HOXD* genes, which was not observed in our 4 ES samples. In addition, WNT and Hedgehog signaling pathways are similarly activated in both BCS and *BCOR* ITD tumors of central nervous system.[1,37,38]

In conclusion, we report a large series of 36 BCS, highlighting the significant morphologic, immunohistochemical and transcriptional overlap with other primitive round/spindle cell sarcomas with *BCOR* gene alterations, despite differences in their demographics and clinical presentations. Our results also show that BCS have histologic features, immunoprofile and expression signatures which are distinct from other common round cell sarcomas, such as ES and *CIC-DUX4* tumors. Emerging evidence suggests that most BCS tumors are chemosensitive to ES-based therapy protocols, although other less toxic regimens currently applied in CCSK might also be investigated. Lastly, the overall survival rate of BCS is significantly more favorable than *CIC*-rearranged sarcomas, but appears similar to ES and SS though long term follow up may be needed.

Supplementary Material

Refer to Web version on PubMed Central for supplementary material.

Acknowledgments

The authors are grateful to the following pathologists for submitting the cases and clinical information when available: Dr. A. Jennifer, Vellore, India (2 cases); Dr. E. Zambrano, Stanford, CA; Dr. J. McKenney, Cleveland, OH; Dr. H. Haddad, Amman, Jordan; Dr. N. Dave, Indianapolis, IN; Drs. H-K Park and Y.L. Choi, Seoul, Korea; Dr. D. Creytens, Gent, Belgium; Dr. E. Vlodavsky, Haifa, Israel; Dr. P. Ferguson, Toronto, Canada.

Supported in part by: P50 CA140146-01 (CRA); P30 CA008748 (CRA); Kristen Ann Carr Foundation (CRA); Cycle for Survival (CRA)

References

1. Pierron G, Tirode F, Lucchesi C, et al. A new subtype of bone sarcoma defined by BCOR-CCNB3 gene fusion. Nat Genet. 2012; 44:461–466. [PubMed: 22387997]
2. Puls F, Niblett A, Marland G, et al. BCOR-CCNB3 (Ewing-like) sarcoma: a clinicopathologic analysis of 10 cases, in comparison with conventional Ewing sarcoma. Am J Surg Pathol. 2014; 38:1307–1318. [PubMed: 24805859]
3. Peters TL, Kumar V, Polikepahad S, et al. BCOR-CCNB3 fusions are frequent in undifferentiated sarcomas of male children. Mod Pathol. 2015; 28:575–586. [PubMed: 25360585]
4. Kao YC, Sung YS, Zhang L, et al. Recurrent BCOR Internal Tandem Duplication and YWHAE-NUTM2B Fusions in Soft Tissue Undifferentiated Round Cell Sarcoma of Infancy: Overlapping Genetic Features With Clear Cell Sarcoma of Kidney. Am J Surg Pathol. 2016; 40:1009–1020. [PubMed: 26945340]
5. Li WS, Liao IC, Wen MC, et al. BCOR-CCNB3-positive soft tissue sarcoma with round-cell and spindle-cell histology: a series of four cases highlighting the pitfall of mimicking poorly differentiated synovial sarcoma. Histopathology. 2016; 69:792–801. [PubMed: 27228320]
6. Argani P, Kao YC, Zhang L. Primary Renal Sarcomas with BCOR-CCNB3 Gene Fusion. A report of 2 cases showing histologic overlap with clear cell sarcoma of kidney, suggesting further link between BCOR-related sarcomas of the kidney and soft tissues. Am J Surg Pathol. 2017 [In Press].
7. Kao YC, Sung YS, Zhang L, et al. BCOR upregulation in a poorly differentiated synovial sarcoma with SS18L1-SSX1 fusion-A pathologic and molecular pitfall. Genes Chromosomes Cancer. 2017; 56:296–302. [PubMed: 27914109]
8. Nakayama R, Mitani S, Nakagawa T, et al. Gene expression profiling of synovial sarcoma: distinct signature of poorly differentiated type. Am J Surg Pathol. 2010; 34:1599–1607. [PubMed: 20975339]
9. Antonescu CR, Owosho AA, Zhang L, et al. Sarcomas With CIC-rearrangements Are a Distinct Pathologic Entity With Aggressive Outcome: A Clinicopathologic and Molecular Study of 115 Cases. Am J Surg Pathol. 2017; 41:941–949. [PubMed: 28346326]
10. Owosho AA, Estilo CL, Rosen EB, et al. A clinicopathologic study on SS18 fusion positive head and neck synovial sarcomas. Oral Oncol. 2017; 66:46–51. [PubMed: 28249647]
11. Specht K, Zhang L, Sung YS, et al. Novel BCOR-MAML3 and ZC3H7B-BCOR Gene Fusions in Undifferentiated Small Blue Round Cell Sarcomas. Am J Surg Pathol. 2016
12. Cohen-Gogo S, Cellier C, Coindre JM, et al. Ewing-like sarcomas with BCOR-CCNB3 fusion transcript: a clinical, radiological and pathological retrospective study from the Societe Francaise des Cancers de L'Enfant. Pediatr Blood Cancer. 2014; 61:2191–2198. [PubMed: 25176412]
13. Shibayama T, Okamoto T, Nakashima Y, et al. Screening of BCOR-CCNB3 sarcoma using immunohistochemistry for CCNB3: A clinicopathological report of three pediatric cases. Pathol Int. 2015; 65:410–414. [PubMed: 26037154]
14. Huynh KD, Fischle W, Verdin E, et al. BCoR, a novel corepressor involved in BCL-6 repression. Genes Dev. 2000; 14:1810–1823. [PubMed: 10898795]

15. Gao Z, Zhang J, Bonasio R, et al. PCGF homologs, CBX proteins, and RYBP define functionally distinct PRC1 family complexes. Mol Cell. 2012; 45:344–356. [PubMed: 22325352]
16. Junco SE, Wang R, Gaipa JC, et al. Structure of the polycomb group protein PCGF1 in complex with BCOR reveals basis for binding selectivity of PCGF homologs. Structure. 2013; 21:665–671. [PubMed: 23523425]
17. Wong SJ, Gearhart MD, Taylor AB, et al. KDM2B Recruitment of the Polycomb Group Complex, PRC1.1, Requires Cooperation between PCGF1 and BCORL1. Structure. 2016; 24:1795–1801. [PubMed: 27568929]
18. Panagopoulos I, Thorsen J, Gorunova L, et al. Fusion of the ZC3H7B and BCOR genes in endometrial stromal sarcomas carrying an X;22-translocation. Genes Chromosomes Cancer. 2013; 52:610–618. [PubMed: 23580382]
19. Antonescu CR, Sung YS, Chen CL, et al. Novel ZC3H7B-BCOR, MEAF6-PHF1, and EPC1-PHF1 fusions in ossifying fibromyxoid tumors--molecular characterization shows genetic overlap with endometrial stromal sarcoma. Genes Chromosomes Cancer. 2014; 53:183–193. [PubMed: 24285434]
20. Yamamoto Y, Tsuzuki S, Tsuzuki M, et al. BCOR as a novel fusion partner of retinoic acid receptor alpha in a t(X;17)(p11;q12) variant of acute promyelocytic leukemia. Blood. 2010; 116:4274–4283. [PubMed: 20807888]
21. Yamamoto Y, Abe A, Emi N. Clarifying the impact of polycomb complex component disruption in human cancers. Mol Cancer Res. 2014; 12:479–484. [PubMed: 24515802]
22. Seki M, Nishimura R, Yoshida K, et al. Integrated genetic and epigenetic analysis defines novel molecular subgroups in rhabdomyosarcoma. Nat Commun. 2015; 6:7557. [PubMed: 26138366]
23. Ng D, Thakker N, Corcoran CM, et al. Oculofaciocardiodental and Lenz microphthalmia syndromes result from distinct classes of mutations in BCOR. Nat Genet. 2004; 36:411–416. [PubMed: 15004558]
24. Nguyen TB, Manova K, Capodieci P, et al. Characterization and expression of mammalian cyclin b3, a prepachytene meiotic cyclin. J Biol Chem. 2002; 277:41960–41969. [PubMed: 12185076]
25. Kao YC, Sung YS, Zhang L, et al. BCOR Overexpression Is a Highly Sensitive Marker in Round Cell Sarcomas With BCOR Genetic Abnormalities. Am J Surg Pathol. 2016
26. Ueno-Yokohata H, Okita H, Nakasato K, et al. Consistent in-frame internal tandem duplications of BCOR characterize clear cell sarcoma of the kidney. Nat Genet. 2015; 47:861–863. [PubMed: 26098867]
27. Foo WC, Cruise MW, Wick MR, et al. Immunohistochemical staining for TLE1 distinguishes synovial sarcoma from histologic mimics. Am J Clin Pathol. 2011; 135:839–844. [PubMed: 21571956]
28. Magro G, Salvatorelli L, Alaggio R, et al. Diagnostic utility of cyclin D1 in the diagnosis of small round blue cell tumors in children and adolescents. Hum Pathol. 2017; 60:58–65. [PubMed: 27984122]
29. Hung YP, Fletcher CD, Hornick JL. Evaluation of ETV4 and WT1 expression in CIC-rearranged sarcomas and histologic mimics. Mod Pathol. 2016; 29:1324–1334. [PubMed: 27443513]
30. Righi A, Gambarotti M, Longo S, et al. Small cell osteosarcoma: clinicopathologic, immunohistochemical, and molecular analysis of 36 cases. Am J Surg Pathol. 2015; 39:691–699. [PubMed: 25723116]
31. Hamilton SN, Carlson R, Hasan H, et al. Long-term Outcomes and Complications in Pediatric Ewing Sarcoma. Am J Clin Oncol. 2017; 40:423–428. [PubMed: 25599318]
32. Argani P, Perlman EJ, Breslow NE, et al. Clear cell sarcoma of the kidney: a review of 351 cases from the National Wilms Tumor Study Group Pathology Center. Am J Surg Pathol. 2000; 24:4–18. [PubMed: 10632483]
33. Furtwangler R, Gooskens SL, van Tinteren H, et al. Clear cell sarcomas of the kidney registered on International Society of Pediatric Oncology (SIOP) 93-01 and SIOP 2001 protocols: a report of the SIOP Renal Tumour Study Group. Eur J Cancer. 2013; 49:3497–3506. [PubMed: 23880476]
34. Pearson JC, Lemons D, McGinnis W. Modulating Hox gene functions during animal body patterning. Nat Rev Genet. 2005; 6:893–904. [PubMed: 16341070]

35. Rux DR, Wellik DM. Hox genes in the adult skeleton: Novel functions beyond embryonic development. Dev Dyn. 2017; 246:310–317. [PubMed: 28026082]

36. Bhatlekar S, Fields JZ, Boman BM. HOX genes and their role in the development of human cancers. J Mol Med (Berl). 2014; 92:811–823. [PubMed: 24996520]

37. Sturm D, Orr BA, Toprak UH, et al. New Brain Tumor Entities Emerge from Molecular Classification of CNS-PNETs. Cell. 2016; 164:1060–1072. [PubMed: 26919435]

38. Paret C, Theruvath J, Russo A, et al. Activation of the basal cell carcinoma pathway in a patient with CNS HGNET-BCOR diagnosis: consequences for personalized targeted therapy. Oncotarget. 2016; 7:83378–83391. [PubMed: 27825128]

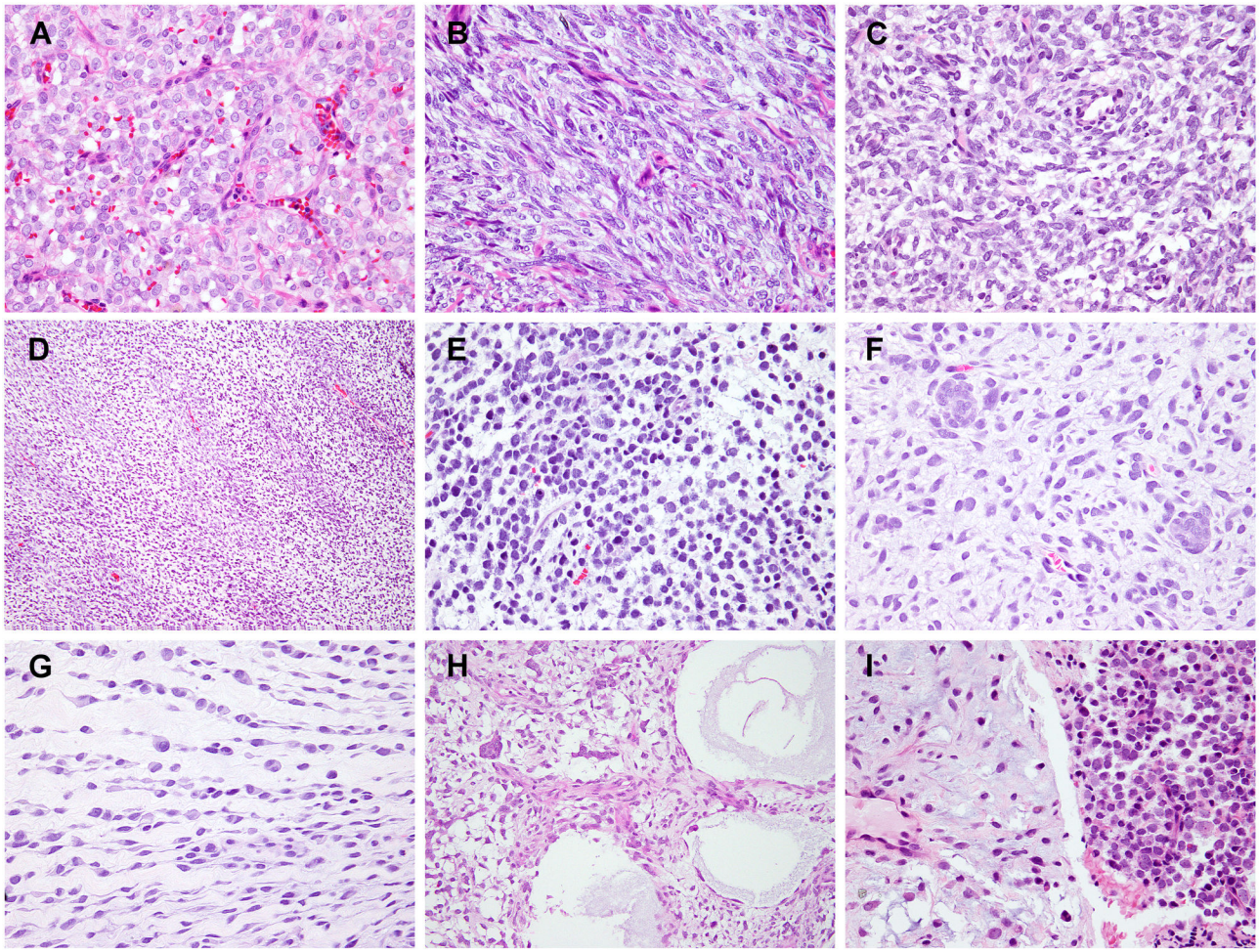

Figure 1. Histologic spectrum of BCS with round to spindle cells and occasional myxoid stroma

(A) A predominant round cell morphology with uniform nuclei, fine chromatin pattern, and delicate vascular network;

(B) Monomorphic spindle cell morphology arranged in a fascicular pattern, reminiscent of SS;

(C) Short spindle to ovoid cells with vague whorling pattern;

(D) Alternating hypercellular and hypocellular areas, mimicking MPNST.

(E) Small amount of myxoid stroma between loosely arranged tumor cells is a common finding.

(F–H) Less common features includes: cell clustering (F), cord-like arrangement (G), and microcystic formation (H);

(I) Sharp contrast of hypercellular round cell component and hypocellular myxoid area

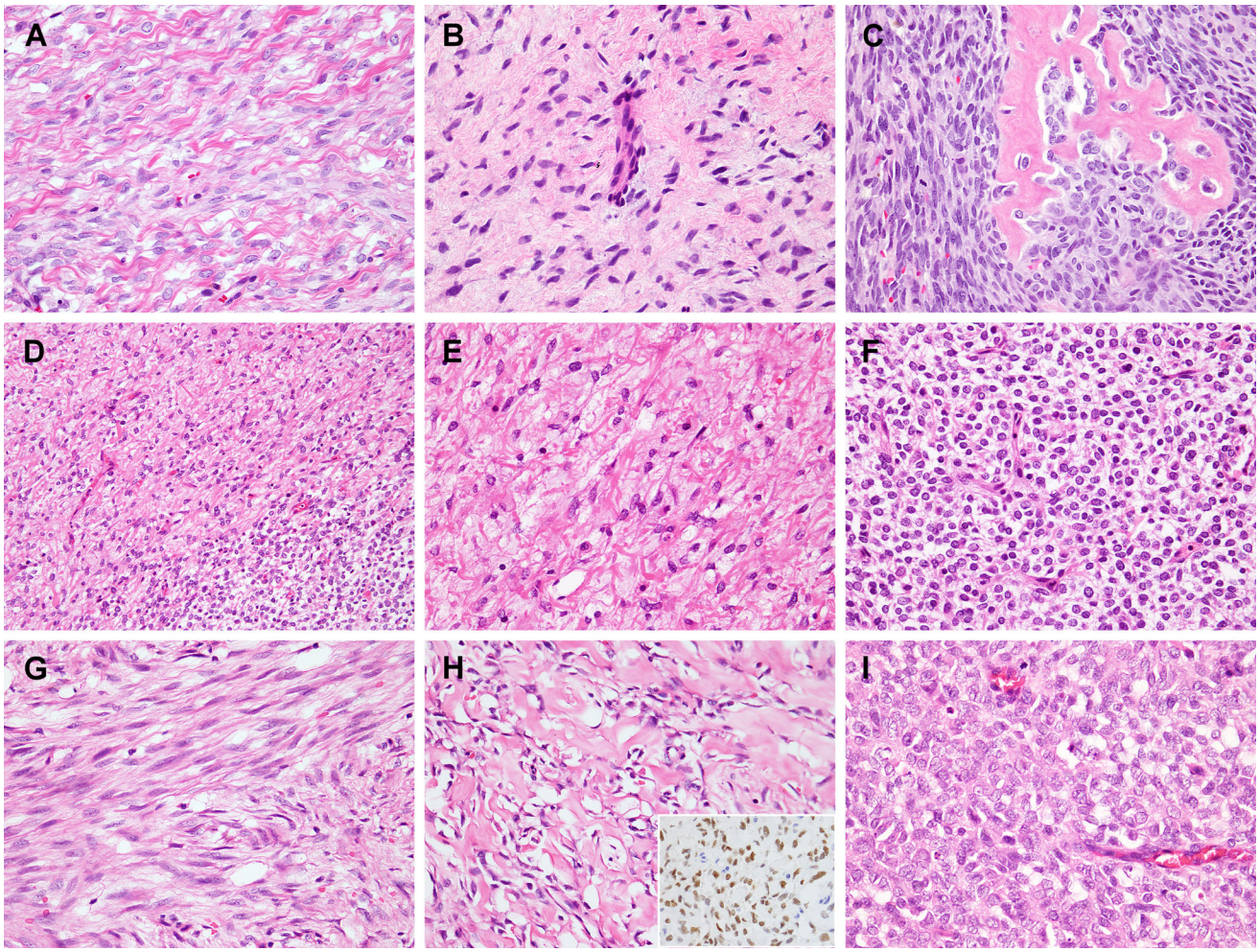

Figure 2. Infrequent morphologic patterns of BCS

(A) Ropey collagen fibers separating spindle tumor cells.

(B) A more homogenous, silky collagenous background with scattered short spindle cells.

(C) Osteoid matrix deposition in a metastatic lung lesion, but not in the primary tumor.

(D–F) A chest wall tumor of a 15 year-old male shows alternating areas of hypocellular collagenous background (D, left upper; E) and hypercellular round cell component (D, right lower; F)(case 23).

(G–I) A foot mass of a 14 year-old male shows a purely spindle cell tumor with low to intermediate cellularity (G) and thick hyalinized collagen (H) in the primary lesion (case 20). Local recurrences 1 year and 3 years later showed a predominant round cell morphology (I). Both the primary and recurrent specimens were positive for *BCOR-CCNB3* fusion by FISH. BCOR IHC showed patchy moderate to strong staining in the primary lesion (H, inset).

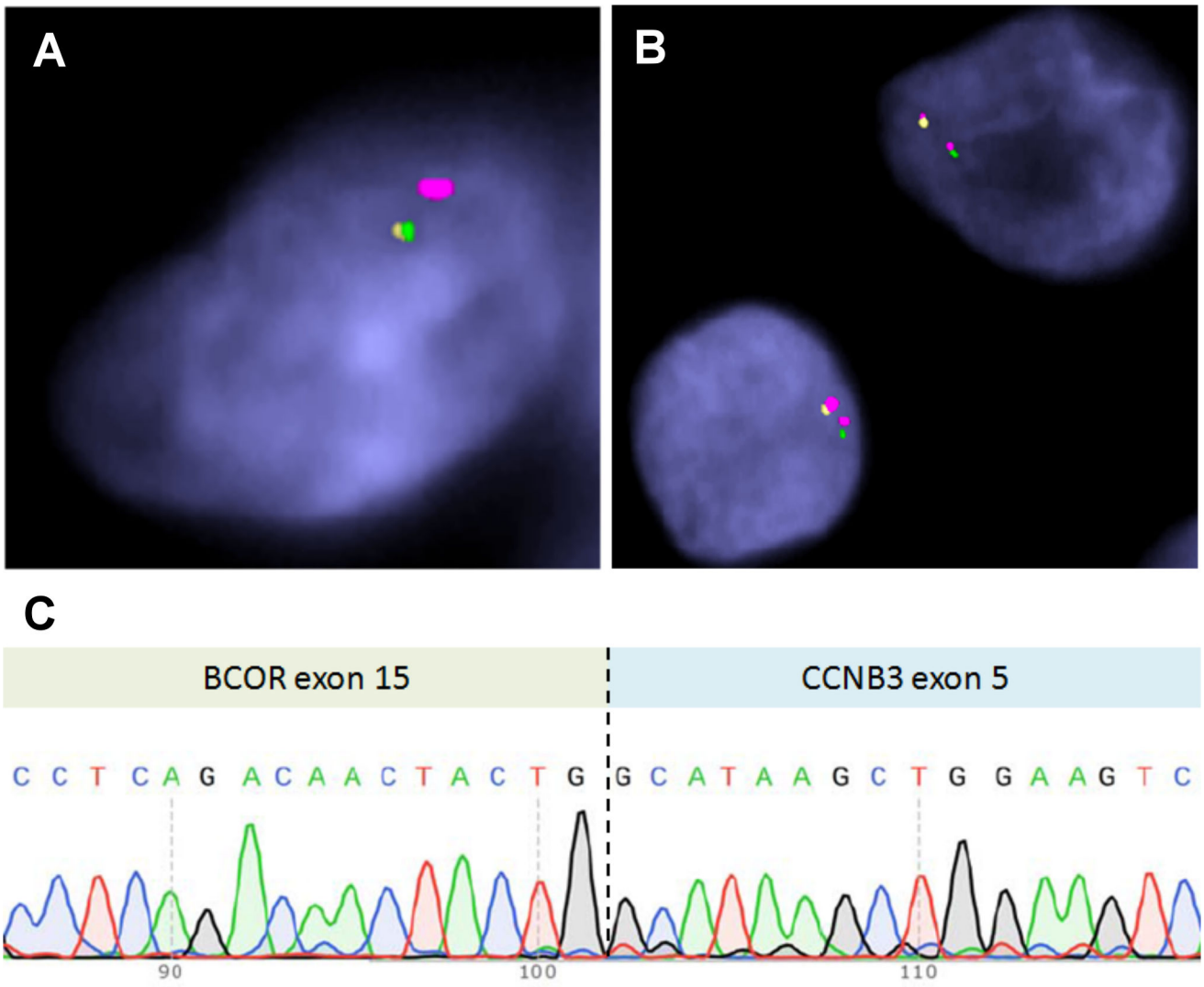

Figure 3. FISH and RT-PCR testing for *BCOR-CCNB3* fusions

(A) Normal signal pattern: green and yellow signal probes flanking telomeric and centromeric ends of *BCOR*, respectively, while red signals flank *CCNB3* on each side. (B) Abnormal FISH pattern: green and yellow signals show break-apart, while red signals split into two signals, representing centromeric and telomeric *CCNB3* signals. A *BCOR-CCNB3* fusion is confirmed when the yellow (centromeric *BCOR*, 5') comes together with one of the red signals. (C) Sanger sequencing of RT-PCR product showed *BCOR* exon 15 fused to *CCNB3* exon 5.

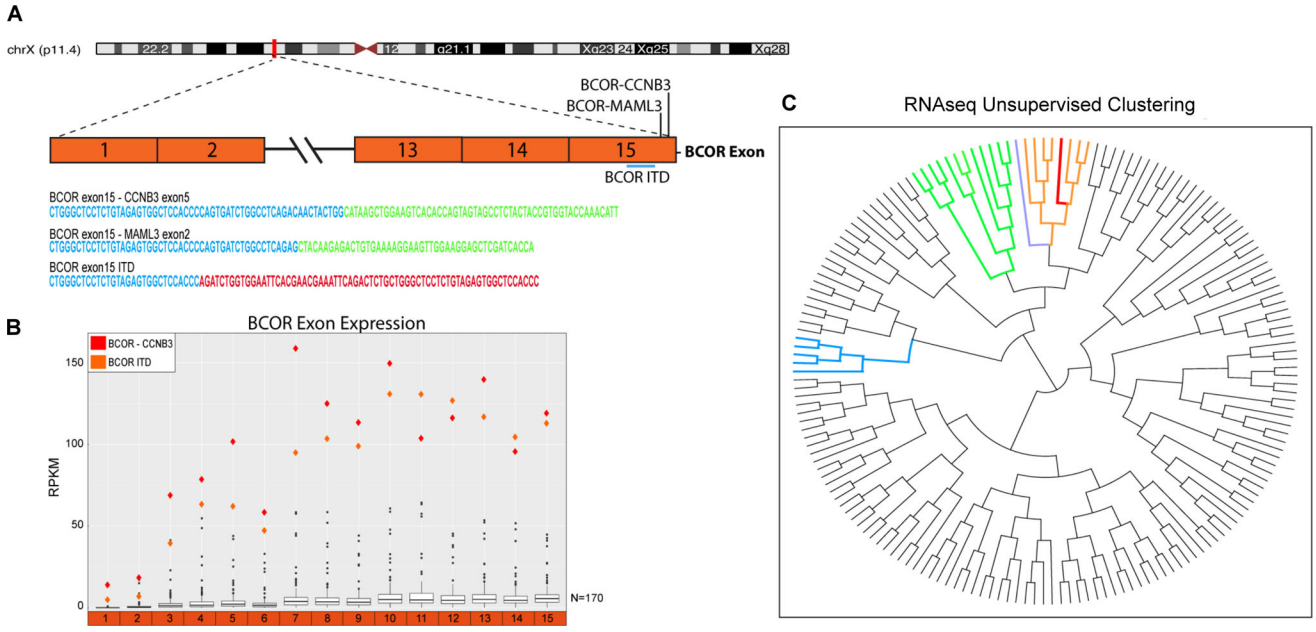

Figure 4. '*BCOR* family of tumor'

(A) Schematic diagram showing *BCOR-CCNB3, BCOR-MAML3* fusions, and *BCOR* ITD (common duplicated region underlined) involving the last exon (exon 15) of *BCOR.* Representative sequences from RNAseq data demonstrating the alterations of *BCOR* (in blue) only a few nucleotides away from each other. (B) At exon level, up-regulations of *BCOR* in *BCOR-CCNB3* (red) and *BCOR* ITD (orange) are observed up to the last exon, consistent with the genetic change at the end of exon 15. Black dots indicate other soft tissue tumors in the same platform as control. (C) Unsupervised clustering using RNAseq data shows clustering of *BCOR-CCNB3* sample (red) with *BCOR* ITD (orange) and *BCOR-MAML3* (purple) into a group, separate from Ewing sarcomas (blue) and *CIC*-rearranged sarcomas (green).

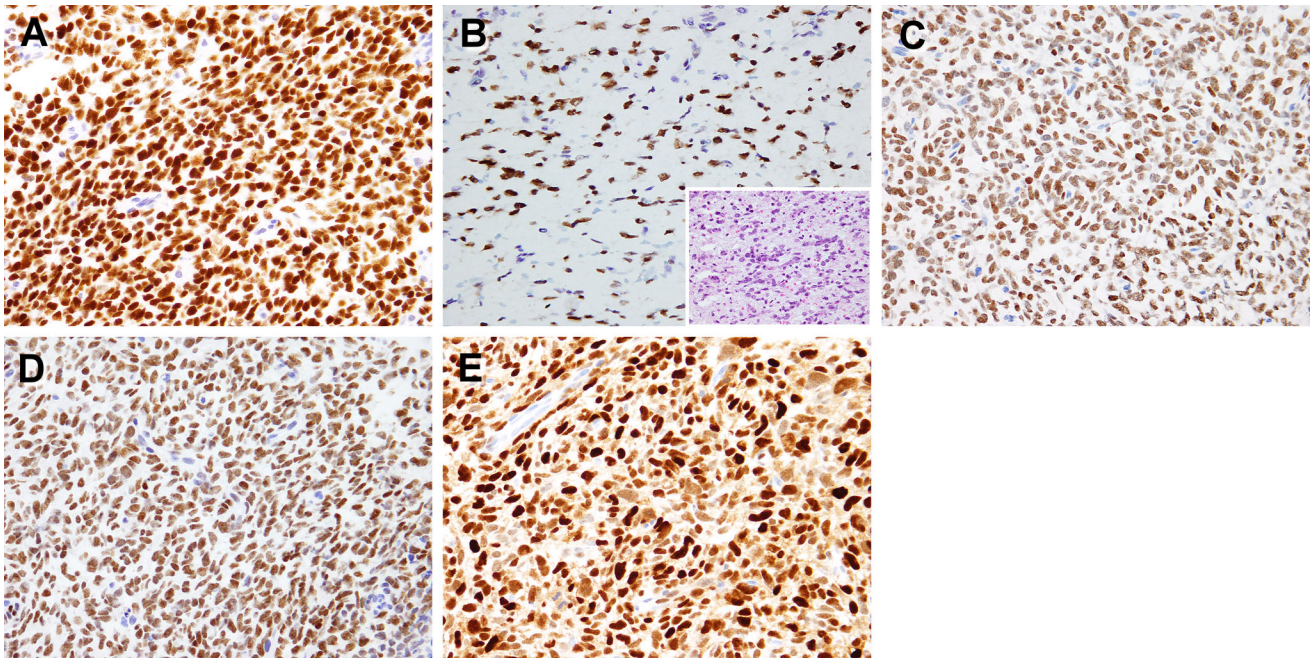

Figure 5. Immunohistochemistry of *BCOR-CCNB3* tumors

(A) BCOR staining is typically diffuse with a strong nuclear pattern. (B) Post-chemotherapy resection of case 7 showing 90% tumor necrosis and foci of residual viable tumor cells (inset) with retained BCOR staining. SATB2 (C), TLE1 (D), and cyclin D1 (E) are also expressed in the majority of cases.

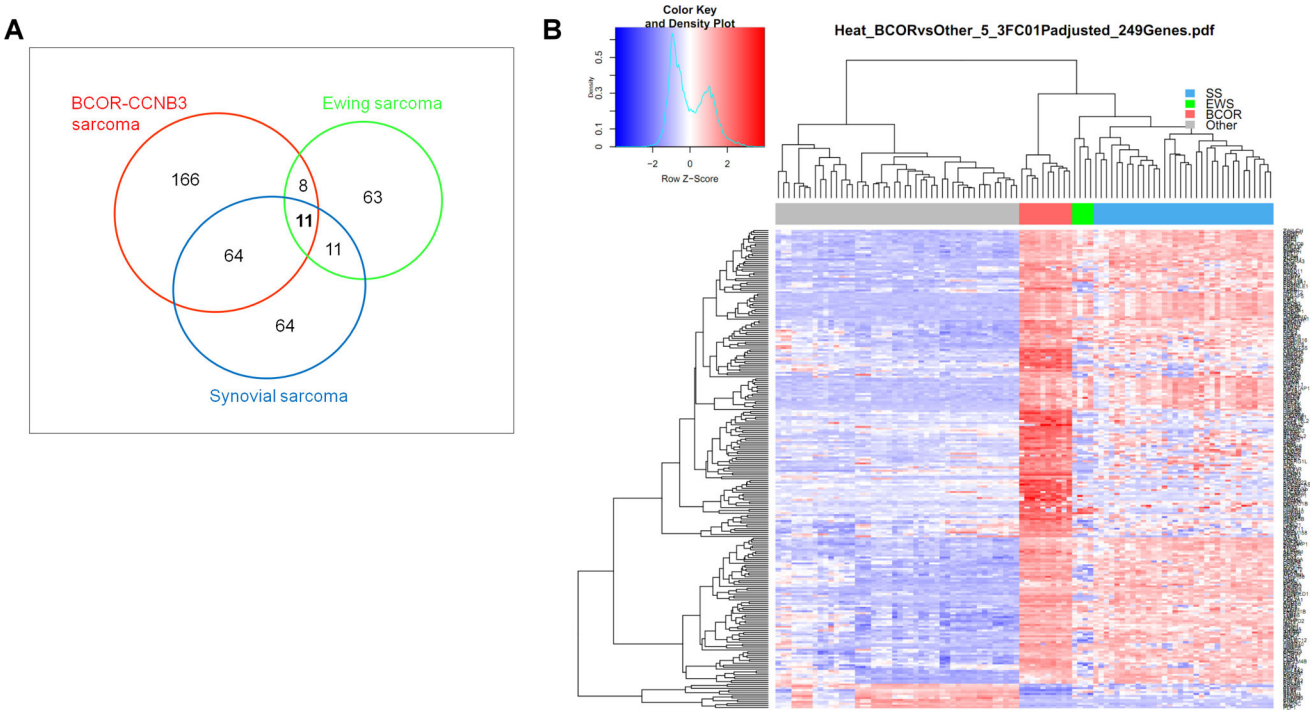

Figure 6.

(A) Venn diagram showed limited transcriptional overlap between BCS, ES, and SS gene (11 genes in common). Additionally, 64 genes were shared between BCS and SS, and 8 genes between BCS and ES. (B) Supervised clustering using the BCS gene signature showed that ES (green), BCS (red), and most SS (blue) samples clustered into distinct individual clusters.

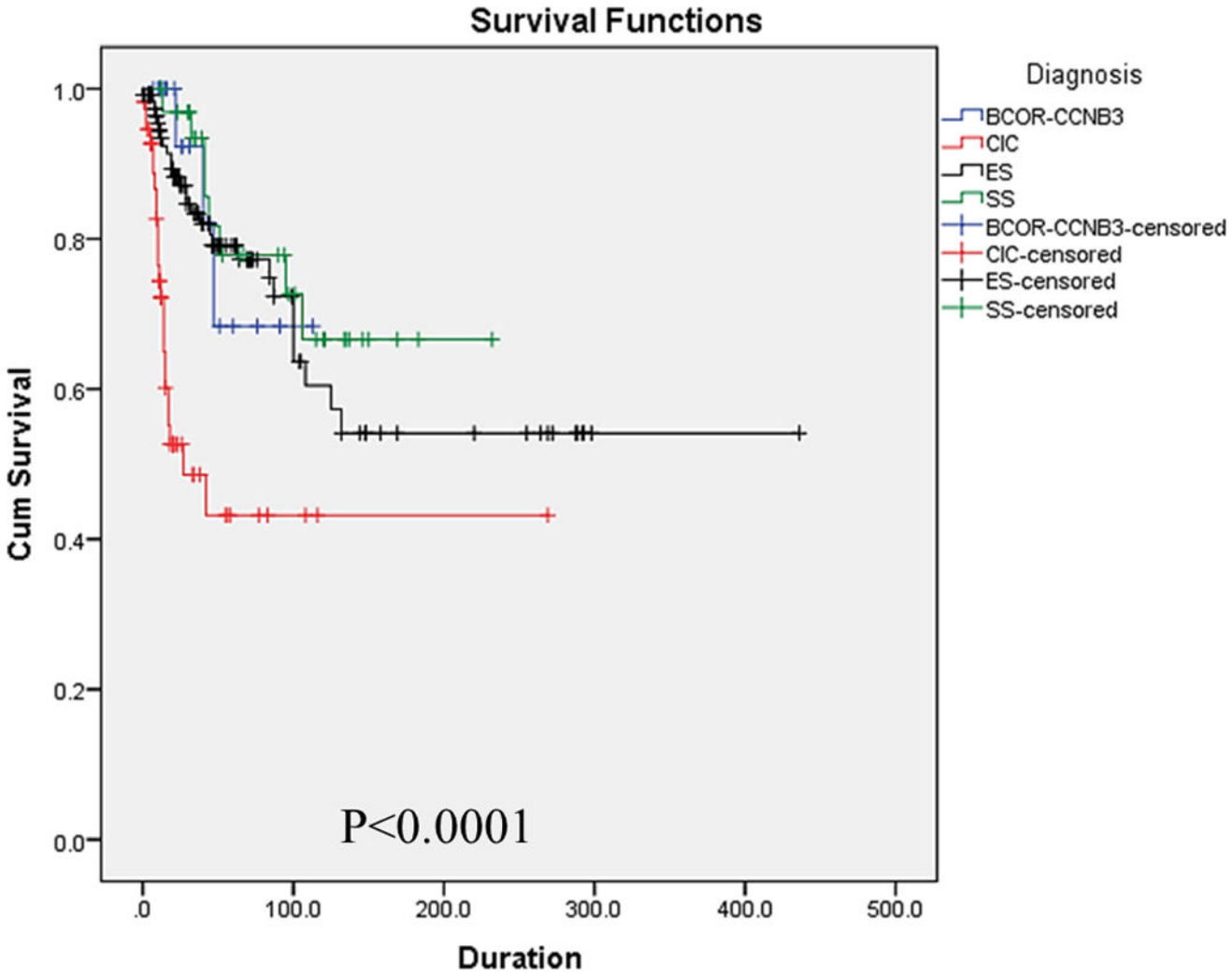

Figure 7.

Overall survival of 22 BCS (blue), 121 ES (black), 34 SS (green), and 57 *CIC*-rearranged sarcomas (red). BCS was associated with a more favorable outcome compared to *CIC*-rearranged sarcoma (p=0.005), while no significant survival difference was noted between BCS and ES (p=0.738) or BCS and SS (p=0.802). Duration is shown in months.

Table 1

Clinicopathologic factors and follow-up information in *BCOR-CCNB3* sarcoma patients

Case	Age/Sex	Location	Size (cm)	Mitotic rate (/10HPFs)	Surgery	Chemotherapy	RT	TNR	Follow-up (months)	Recurrence & Metastasis (site)
1	13/F	Soft palate	3	NA	YES$^{\Delta}$	(ES)	N	100 (IV)	NED (14)	
2	15/M	Femur	14.5	11	YES$^{\Delta}$	(ES): VAC-IE, IT	N	100 (IV)	NED (43)	
3	15/F	Pelvic cavity	10.3	3	YES$^{\gamma}$	(ES): VAC-IE, IT	Y	95 (III)	NED (76)	
4	9/M	Sacrum	5	10	YES$^{\Delta}$	(ES)	Y	(III)	NED (26)	
5	13/M	Femur	15	1	YES$^{\Delta}$	(OS) then (ES)	N	95 (III)	AWD (60)	R
6	14/M	Iliac bone	16.3	4	YES$^{\Delta}$	(ES): VAC-IE, IT	N	60–70 (II)	NED (11)	
7	2/M	RP/paraspinal	5	18	YES$^{\Delta}$	(ES): VAC-IE, IT	N	80 (II)	DUC (40)	
8	17/M	Pubic ramus	NA	25	YES$^{\Delta}$	(ES) VA-IE	N	40 (I)	AWD (54)	M (pancreas, at diagnosis), R
9	14/M	Foot	NA	3	YES$^{\Delta}$	(ES)	Y	(I)	NA *	Lung nodules
10	15/M	Femur	NA	8	YES$^{\Delta}$	regimen unknown	N	NA	NED (31)	
11	17/M	Calcaneus	15.5	22	YES$^{\gamma}$	MTX, Cp	Y	NA	DOD(47)	R, M (lung, pelvis, scapula, thigh)
12	12/M	Pubic ramus	12	1	YES	(ES)	N	--	NED (51)	
13	5/M	Calcaneus	3.7	4	YES	(ES)	Y	--	NED (10)	
14	18/M	Shoulder	11	16	YES	(ES)	Y	--	NED (7)	
15	18/F	Paraspinal C2–C6	7	3	YES	I, A, Mesna	Y	--	NED (26)	
16	10/M	Femur	8.2	10	YES	I, A	N	--	NED (91)	
17	18/M	Sacrum	7	NA	YES	Er, C, Nedaplastin	Y	--	AWD (16)	
18	44/M	Thigh	14	14	YES	I, Cp	Y	--	DOD (22)	M (lung)
19	18/F	Sacrum	5	8	N	(ES) VAC-IE	Y	--	AWD (113)	R, M (lung, skull base)
20	14/M	Foot	5	1	YES	N	N	--	NED (44)	R
21	12/M	Kidney	13	4	YES	N	N	--	AWD (15)	R
22	2/M	Posterior neck	25	11	YES	N	N	--	AWD (11)	
23	15/M	Chest wall	NA	6	YES	N	N	--	NED (21)	
24	19/M	Pelvic cavity	20	9	YES	NA	NA	--	NA	

Case	Age/Sex	Location	Size (cm)	Mitotic rate (/10HPFs)	Surgery	Chemotherapy	RT	TNR	Follow-up (months)	Recurrence & Metastasis (site)
25	21/M	Chest wall	NA	4	YES	NA	NA	--	NA	
26	24/M	Tibia	11.7	15	YES	NA	NA	--	NA	
27	11/M	Kidney	27	4	YES	NA	NA	--	NA	
28	13/M	Tibia	NA	2	NA	NA	NA	--	NA	
29	15/M	Leg	10	6	NA	NA	NA	--	NA	
30	15/M	Elbow(bone)	NA	1	NA	NA	NA	--	NA	
31	16/M	Tibia	NA	2	NA	NA	NA	--	NA	
32	10/M	Femur	7.8	NA	NA	NA	NA	--	NA	
33	13/M	Tibia	NA	4	Biopsied	NA	NA	--	NA *	
34	15/M	Iliac bone	NA	13	Biopsied	NA	NA	--	NA *	
35	16/M	Calcaneus	NA	3	Biopsied	A, Cp	N	--	NA *	
36	13/F	Back/paraspinal	19.6	2	Biopsied	NA	NA	--	NA *	

HPFs, high power fields; RT, radiation therapy; TNR, tumor necrosis rate; ES, Ewing sarcoma; OS, osteosarcoma; NED, no evidence of disease; AWD, alive with disease; DOD, dead of disease; DUC, dead of unknown cause; NA, not available; V, vincristine; A, doxorubicin/adriamycin; C, cyclophosphamide; I, ifosfamide; E, etoposide; MTX, methotrexate; Cp, cisplatin; Er, epirubicin; R, recurrence; M, metastasis;

Δ, surgery was performed after neoadjuvant chemotherapy;

γ, surgery performed after chemo-radiation;

*, recent case